Multi-scale damage analysis and fatigue behavior of PLA manufactured by fused deposition modeling (FDM)

Hamid Reza Vanaei
Arts et Metiers Institute of Technology, CNAM, LIFSE, HESAM University, Paris, France and Arts et Metiers Institute of Technology, CNRS, CNAM, PIMM, HESAM University, Paris, France
Mohammadali Shirinbayan
Arts et Metiers Institute of Technology, CNRS, CNAM, PIMM, HESAM University, Paris, France
Saeedeh Vanaei
INSA Centre Val de Loire, Blois, France
Joseph Fitoussi
Arts et Metiers Institute of Technology, CNRS, CNAM, PIMM, HESAM University, Paris, France
Sofiane Khelladi
Arts et Metiers Institute of Technology, CNAM, LIFSE, HESAM University, Paris, France, and
Abbas Tcharkhtchi
Arts et Metiers Institute of Technology, CNRS, CNAM, PIMM, HESAM University, Paris, France

Abstract

Purpose – Fused deposition modeling (FDM) draws particular attention due to its ability to fabricate components directly from a CAD data; however, the mechanical properties of the produced pieces are limited. This paper aims to present the experimental aspect of multi-scale damage analysis and fatigue behavior of polylactic acid (PLA) manufactured by FDM. The main purpose of this paper is to analyze the effect of extruder temperature during the process, loading amplitude, and frequency on fatigue behavior.

Design/methodology/approach – Three specific case studies were analyzed and compared with spool material for understanding the effect of bonding formation: single printed filament, two printed filaments and three printed filaments. Specific experiments of quasi-static tensile tests coupled with microstructure observations are performed to multi-scale damage analysis. A strong variation of fatigue strength as a function of the loading amplitude, frequency and extruder temperature is also presented.

Findings – The obtained experimental results show the first observed damage phenomenon corresponds to the inter-layer bonding of the filament interface at the stress value of 40 MPa. For instance, fatigue lifetime clearly depends on the extruder temperature and the loading frequency. Moreover, when the frequency is 80 Hz, the coupling effect of thermal and mechanical fatigue causes self-heating which decreases the fatigue lifetime.

Originality/value – This paper comprises useful data regarding the mechanical behavior and fatigue lifetime of FDM made PLA specimens. In fact, it evaluates the effect of process parameters (extruder temperature) based on the nature of FDM that is classified as a thermally-driven process.

Keywords FDM, Damage, PLA, Fatigue, Inter-layer bonding

1. Introduction

Fused deposition modeling (FDM), an additive manufacturing (AM) process, was patented (Crump, 1991) and developed for modeling and prototyping to produce complex geometries, low cost and easy operation parts (Mohamed *et al.*, 2015; Macdonald *et al.*, 2014; Vanaei *et al.*, 2020). Owing to its specific characteristic by allowing fabrication of complex geometries, it became a well-known and most commonly used technology in recent years (Chua *et al.*, 2010). In FDM, based on the sliced CAD model and the fact that the sequence of deposited layers occurs successively once upon each other's, the mechanism of layer-by-layer deposition takes place by extruding semi-molten thermoplastic materials through a liquefier over a platform (Yagnik, 2014; Chennakesava and Narayan, 2014).

Three-dimensional-printed structures fabricated by FDM process possessed entirely different mechanical properties from those manufactured by other methods. It is widely mentioned

that the mechanical properties of plastic parts are extensively influenced by the mechanism of layer-by-layer deposition (Vanaei *et al.*, 2020b). This particularly exists in FDM that offers a wide range of process parameters affecting the mechanical behavior of manufactured parts (Vanaei *et al.*, 2020c). Although in recent years the knowledge of mechanical characterization of FDM components is barely significant, most studies concentrated on enhancing the strength of materials by preserving the ability to fabricate complex geometry through AM. Consequently, it is stated that there is still a requirement for updating the mechanical strength of these parts.

Meanwhile, there are various studies on thermoplastics such as acrylonitrile butadiene styrene (ABS), polylactic acid (PLA) and polycarbonate (PC) to estimate and analyze their mechanical properties and especially fatigue analysis. They showed that the more density of the parts resulted in more correlation to the traditionally manufactured of the same material. This requires an acceptable orientation to avoid delamination.

According to the above-mentioned point, AM parts offer improvement in fatigue lifetime rather than traditional manufacturing processes (Blattmeier *et al.*, 2012). However, (Van Hooreweder *et al.*, 2013) indicated that fatigue properties of Nylon specimens remained similar in both injection molding and selective laser sintering. It is well-noted that these materials have significantly lower fatigue lifetime compared with others (Brandl *et al.*, 2012; Santos *et al.*, 2002). In fact, there are some parameters that have impact on the mentioned fatigue lifetime; including lack and/or weakness of bonding through the lamination resulted particularly during layer-by-layer deposition mechanism and also the presence of voids (Brandl *et al.*, 2012; Santos *et al.*, 2002; Wang, 2012).

Furthermore, Lee and Huang (2013) investigated on ABS and ABS-plus materials fabricated by FDM process to study the effect of print orientations on fatigue lifetime. On the other hand, another work was performed on ABS-M30i by optimizing process parameters of FDM and applying Taguchi method to determine the tensile strength and surface roughness of the material (Alhubail *et al.*, 2013). A similar work fabricated PC specimens, which was based on the analysis of tensile strength for FDM parts, and they obtained a 75% enhancement in tensile strength comparing to that of the extruded PC parts (Masood *et al.*, 2010). In comparison to others and on the same level to ABS, PLA is a common material in 3D printing. It is stronger than ABS, whereas the ductility is lower. It is a biodegradable thermoplastic made of recyclable sources that do not have a health risk (Stephens *et al.*, 2013). Its high mechanical strength and convincing barrier properties make it important to extend the application of this material. Although several researchers considered the mechanical properties of PLA as a composite comprising many fibers (Dong *et al.*, 2014; Kasuga *et al.*, 2000), other tried to work on the mechanical behavior of PLA by changing the most useful parameters in FDM process (Jerez-Mesa *et al.*, 2017; Averett *et al.*, 2011; Letcher and Waytashek, 2014; Afrose *et al.*, 2016; Susmel, 2014). Despite the variety of published work in the fatigue properties of FDM-processed PLA, it is imperative to have a deeper and more detailed investigation.

Worth mentioning that analyzing the mechanical properties and especially damage mechanism of FDM parts is an important issue. In literature, there are a limited number of works on the damage phenomenon of polymeric parts and exclusively PLA. Moreover, the temperature evolution of deposited filaments is a key parameter and has impact on the bonding quality.

The presented work concentrates on the fatigue properties of PLA by putting through dog-bone samples under cyclic loading. The aim is to analyze the influence of extruder temperature on the mechanical properties of the final sample and also multi-scale damage mechanisms under quasi-static loading-unloading tensile test.

2. Material and experimental methodology

2.1 Polylactic acid filament

A commercially available Pearl Violet PLA filament with a diameter of 1.75 mm has been analyzed, which is manufactured by Fillamentum® (Czech Republic). Some physicochemical properties are presented in Table 1.

2.2 Three-dimensional-printer device

The dog bone specimen was produced using a desktop 3D printer. The pattern for each layer was selected to be printed in 45° to the axis X and Y (90° to each other's), to make sure that each successive layer has enough support on it. Presumably, at 45°, the 3D model is printed properly because every layer is in about 50% contact with the previous layer. The printer fixed in a temperature-controlled atmosphere of the envelope and built the rapid-prototyped (RP) model based on ASTM D638 type IV in layers by using a single nozzle print head. In the experiments reported here, the solid model file exported as a STL format to be loaded into the FlashPrint software which generates the print path. The designed model is demonstrated in Figure 1.

2.3 Methods

2.3.1 Preliminary characterization methods

Microscopic observations were performed using a scanning electronic microscope (HITACHI 4800 SEM) to investigate qualitatively the material microstructure.

To measure the main transition temperatures, thermo-mechanical (DMTA) tests were applied to the samples using DMA Q800 instrument from TA Company. The tests were realized using a standard sample size of 25*10*4 mm^3 at the following condition: temperature range of 40°C to 100°C; frequency 1 Hz; temperature rate 2°C/min.

2.3.2 Mechanical characterization: tensile and fatigue tests

Tensile tests until failure have been carried out at room temperature on MTS 830 hydraulic machine. The printed

Table 1 Physio-chemical properties of PLA filament

Properties	Typical Value
Material density	1.24 g/cm^3
Diameter (Tolerance)	1.75 mm (±0.01 mm)
Glass transition temperature	72°C
Melting temperature	158°C

Figure 1 Test case printed using FlashForge 3D printer (based on ASTM D638 type IV)

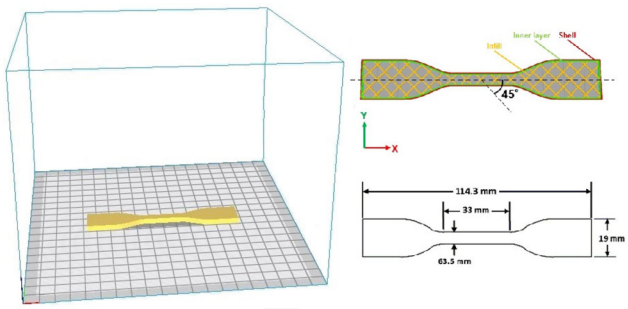

sample (based on ASTM D638 type IV) were used for tensile test with velocity of 1 mm/min. A contactless technique is used to measure the local deformation using a camera. The strain measurement procedure consists of analyzing the images of the filmed surface during deformation.

To understand the effect of bonding formation on the tensile behavior of printed PLA, tensile facts on these filaments are proposed (Figure 2):

- Spool material
- Single printed filament
- Two printed filaments
- Three printed filaments

Tension-tension fatigue tests were carried out at different applied maximum stress on MTS 830 hydraulic fatigue machine using the same standard (ASTM D638 type IV). The minimum applied stress was chosen to be equal to 10% of the maximum applied stress. In this paper, results of the experimental procedure performed at different frequencies of 1, 10 and 80 Hz are presented.

During cyclic loading, the temperature rise (due to self-heating) has been measured using an infrared camera (Raynger-MX4) in a specific area (maximum temperature). The evolution of Young's modulus was also determined.

Figure 2 Proposed printed filaments to perform tensile tests

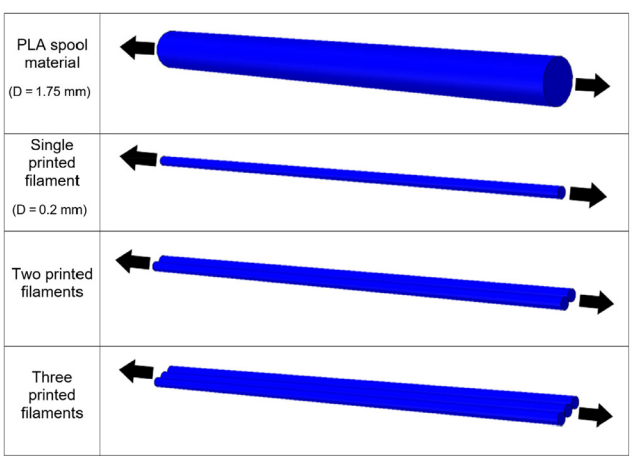

2.4 Conditions of printing

The influence of extruder temperature was taken into account by defining three conditions as displayed in Table 2. Five samples were tested for each condition of tensile tests.

3. Results and discussion

The objective of this study is to analyze the effects of extruder temperature on the mechanical properties and fatigue lifetime of parts produced by FDM process.

3.1 Thermo-mechanical properties

In the presented work, all mechanical tests were performed at room temperature. To measure the main transition temperatures due to molecular mobility as a function of temperature, DMTA tests were used. The graph presented in Figure 3 clearly displays the evolution of the storage and loss modulus versus temperature obtained by the DMTA test. Apparently, PLA filament presents at least three distinct zones in the temperature range of 40°C-100°C. The first zone, extended until 60°C, is the glassy state. The second zone is related to the glass transition zone. From 80°C the rubbery state appeared.

According to the mentioned graph and data extracted by monitoring the temperature during the fatigue test, the temperature growth (self-heating) during the test will not exceed 50°C. Otherwise, the thermal fatigue will be intervened.

3.2 Tensile behavior

3.2.1 Polylactic acid filaments

Figure 4 depicts the results of tensile tests at room temperature for the set of specimens investigated in this study. These results have surprisingly referenced the nature of FDM process. Regardless of the variation in failure strain for the four specimens (PLA spool material, one printed filament, two printed filaments and three printed filaments), no significant difference observed in Young's modulus. Apparently, the

Table 2 Various conditions of printing

Condition no.	Extruder Temperature (°C)	Bed Temperature (°C)	Speed (mm/s)	Layer height (mm)
1	210	70	40	0.2
2	220	70	40	0.2
3	230	70	40	0.2

Figure 3 DMTA test result

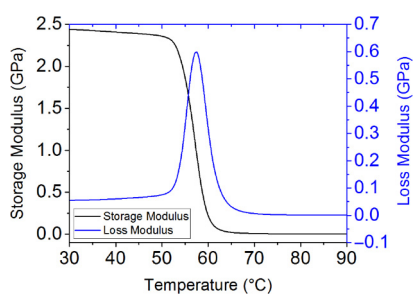

Figure 4 Tensile curves of different formed filaments

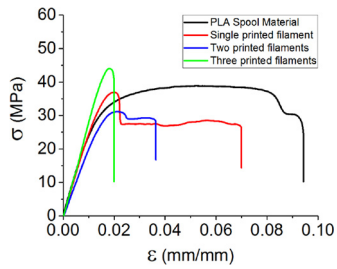

remarkable failure strain in the case of raw material is a notable issue in the assessment of the mechanical behavior of 3D-printed parts.

It seems barely incredible that by increasing the printed layer, the failure strain was decreased about 70%. Conversely, there was a significant increase in the maximum stress up to 20%. It could be argued that the mentioned observations well confirms the brittle behavior of PLA filament after printing. As an example, the failure strain of PLA spool (~9.5%) is almost 4.75 times greater than that of three printed filaments (~2%).

This approach could be a confirmation to the underlying assumption that in the additively manufactured polymer being tested, the mechanical behavior (and in particular the elongation) in the incipient failure condition was markedly affected by the mechanism of layer-by-layer deposition.

3.2.2 Effect of extruder temperature on the tensile behavior

Contrary to the tensile behavior of the progressively printed filaments (Section 3.2.1), different behavior was detected in the samples printed according to the conditions presented in Table 2. To have a more clear precision on the characterization of the fabricated samples, tensile tests were applied at least five times on the samples per each condition. Figure 5 presents the tensile behavior for the set of five specimens assessed according to condition No. 1 (T_{ext} = 210°C). One explanation might be the fact that rupture occurred at the center of the specimens (activate zone of tensile loading). Another convincing point was the repeatability of the set of specimens by the occurrence of rupture at the center of them, as well as the fact that the failure mode was due to the material departure in a plane almost normal to the tensile stress.

Given the above-mentioned results and following the discussion performed on the mechanical behavior, tensile tests have been realized to illustrate the effect of extruder temperature on the tensile behavior. The graph presented in

Figure 5 Tensile behavior for the set of five sample according to the condition No. 1 at T_{ext} = 210°C

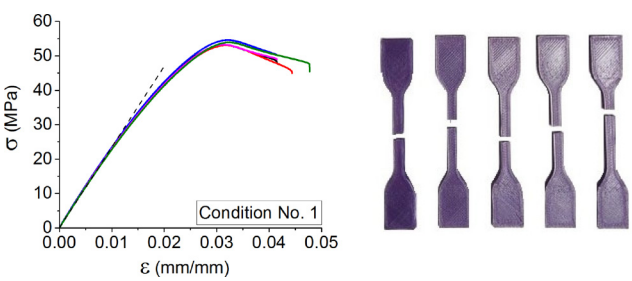

Figure 6 Tensile behavior of printed PLA samples from condition No. 1 to 3

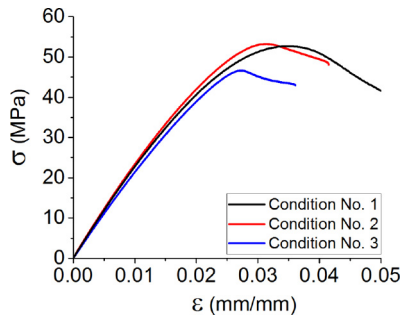

Figure 6 and data collected in Table 3, clearly display and compare the overall results as follows:

- Influence of the extruder temperature on Young's modulus is limited. It roughly changed from 2.3 GPa to 2.5 GPa as the extruder temperature increased from 210°C to 220°C.
- By variation of T_{ext} from 220°C to 230°C, a sudden drop observed below to that of the T_{ext} = 210°C.
- Failure stress changed periodically from 52 MPa to 53 MPa and then 47 MPa by the increase in T_{ext} based on the conditions No. 1-3.
- Failure strain stayed around 3.5% as the T_{ext} decreased from 230°C to 220°C, at T_{ext} = 210°C.
- By comparing the tensile results obtained on filaments and those observed on the set of samples in three conditions, both failure stress and strain dramatically increased.

SEM micrographs of a fractured sample of condition No. 2 are presented in Figure 7. Logically, by increasing the distance from the envelope, the temperature gradient decreases and causes inhomogeneity of the cooling rate of successively deposited filaments. It is probably true to say that based on Figure 7(a), a deformed zone was observed. There is convincing evidence since the surface fracture depicted in Figure 7(b) with the void sequences of upper layers. Presumably, the fracture path proceeded over weak inter-layers bonding.

3.3 Multi-scale damage investigation

Experimental stress-strain curves for quasi-static tensile tests coupled with microstructure observations are shown in Figure 8. The same representative observation zone was microscopically analyzed at consecutive increasing value of applied stress level. The local investigation was assumed as a statistical representative of the damage accumulation in the studied material. Furthermore, microscopic observations have confirmed that this zone is statistically representative of the

Table 3 Results of tensile behavior of printed PLA samples from condition No. 1 to 3

Samples	E (GPa)	σ_{max} (MPa)	ε at σ_{max} (%)
Condition no. 1	2.3 ± 0.1	52 ± 2	3.5 ± 0.3
Condition no. 2	2.5 ± 0.1	53 ± 1.5	3.5 ± 0.2
Condition no. 3	2.2 ± 0.1	47 ± 2	2.7 ± 0.2

Figure 7 SEM micrograph for a) external surface and b) surface fracture of the specimen in condition No. 2

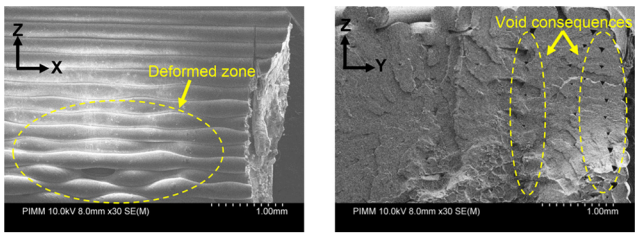

(a) (b)

Figure 8 Damage mechanisms under quasi-static loading

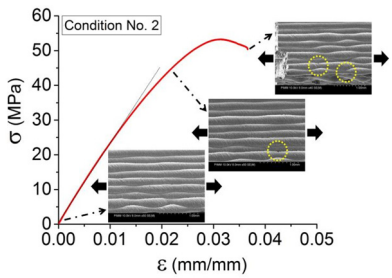

damage accumulation. The first observed damage phenomenon corresponds to the inter-layer failure of the filament interface at the stress value of 40 MPa. This phenomenon is the predominant damage mechanism for quasi-static loading.

Filaments oriented perpendicularly to the principal stress direction are submitted to a high local normal stress at the interface.

To clarify the mentioned issue, a "quantitative multi-scale analysis" of damage effect was performed in this section. At the macroscopic scale, the evolution of stiffness reduction is determined for PLA samples printed from condition No. 2 under quasi-static loading. Stiffness reduction is an appropriate macroscopic damage indicator to express the damage development in materials. In the case of tensile loading, one can define a macroscopic damage variable as:

$$D = 1 - E_D/E_0, \tag{1}$$

where E_0 and E_D are Young's modulus of virgin and the damaged material, respectively. The graph shown in Figure 9 provides the evolution of the macroscopic damage parameter, D, under quasi-static loading-unloading tensile test as a function of applied stress. It should be indicated that for each microstructure, several tests (at least 3) were performed and the results have been reported in this figure in such a way that at least 15 points have been measured until the very last stages just before failure. Figure 9 shows the damage threshold in the term of stress is almost about 35 MPa. Seemingly, an altered slope of the curve (from D = 0.12) signifying the saturation of the filaments interface failure occurring together, with the beginning of the propagation of transverse cracks.

Figure 9 a) Applied stress for PLA printed from condition No. 2 and b) macroscopic damage evolution

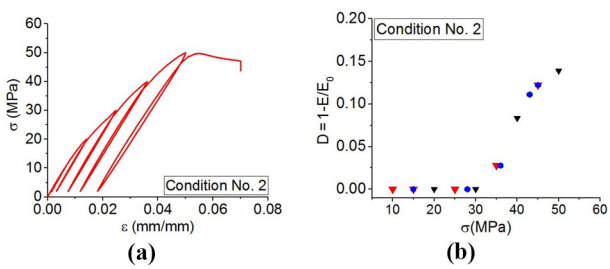

(a) (b)

3.4 Fatigue behavior analysis

3.4.1 Effect of the extruder temperature

Figure 10 shows the Wöhler curve obtained in tension-tension fatigue tests for a frequency of

1 Hz in the case of the samples tested from conditions No. 1, 2 and 3. The diagram shows that for the three cases at high applied stresses, the same fatigue lifetime was observed. However, at low amplitudes, there is a significant difference in fatigue lifetime. In the case of samples printed according to condition No. 3, the fatigue lifetime is about 7×10^3 cycles for applied stress (30 MPa), while the fatigue lifetime is about 2×10^4 cycles for sample printed according to condition No. 2. So, a variation of 10°C on extruder temperature leads to a fatigue lifetime three times greater. Figure 10 confirms that the samples printed according to condition No. 2 represented acceptable fatigue properties.

Thus, the fatigue lifetime at low amplitudes is strongly influenced by the temperature of extruder. Regarding fatigue results at a frequency of 1 Hz, Figure 10 shows a linear curve. In this case, the high loading amplitude zone corresponds to loading amplitude up to 35 MPa. This upper zone corresponds to fatigue lifetime less than 2,000 cycles. Fatigue behavior and specialty S-N curve of PLA printed using FDM process could be modeled by a logarithmic linear expression:

$$\sigma_{max} = A.Ln(N) + B, \tag{2}$$

where A and B are the material parameters corresponding to the slope of the curve and the Y-intercept, respectively. The slope A defines the sensitivity of the fatigue resistance and intercept B represents the apparent tensile strength. Data gathered in Table 4 shows the value of A and B for three conditions of printing related to high and low-stress domains.

Figure 10 Wöhler curves for PLA printed at the three conditions mentioned in Table 2 at 1 Hz

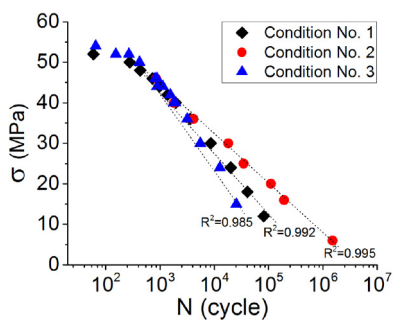

Table 4 Values of a and B

Samples	Low stress domain		High stress domain	
	A (MPa)	B (MPa)	A (MPa)	B (MPa)
Condition no. 1	−6.19	91.66	−0.86	55.95
Condition no. 2	−5.22	79.95		
Condition no. 3	−8.67	104.78		

The evolution of the relative Young's modulus is followed to describe quantitatively the degree of fatigue damage. It may be used in a stiffness-based fatigue failure criterion. Figure 11 shows the evolution of the relative Young's modulus for two applied maximum stresses equal to 18 MPa and 46 MPa corresponding to low and high amplitudes, respectively. These results confirm that for three conditions of printing, the same evolution of relative Young's modulus could be observed at high amplitudes [Figure 11(b)]. It can confirm the same damage mechanism. Believably, the extruder temperature has no effect on the relative Young's modulus evolution while it can affect the fatigue lifetime [Figure 11(a)]. In addition, the graph highlighted the fact that there is no significant damage at low amplitudes just before the failure of the samples while it is more significant at high fatigue amplitudes.

SEM fractography after fatigue tests has been performed to understand the difference between low loading amplitudes (Figure 12). SEM analysis, in the case of a sample printed according to condition No. 2, highlighted that there is a remarkable bonding formation associated with condition No. 3.

Figure 11 Evolutions of the relative Young's modulus (E/E_0) during fatigue tests of three conditions: (a) σ_{max} = 18 MPa and (b) σ_{max} = 46 MPa

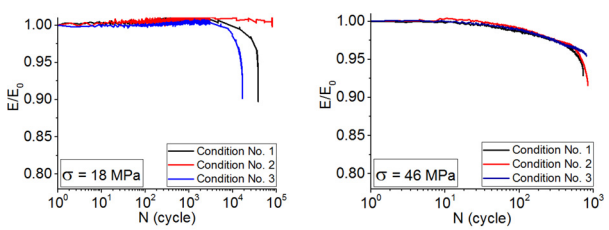

Figure 12 SEM micrographs after fatigue tests at 1 Hz and σ_{max} = 18 MPa for PLA samples printed according to (a) condition No. 2 and (b) condition No. 3

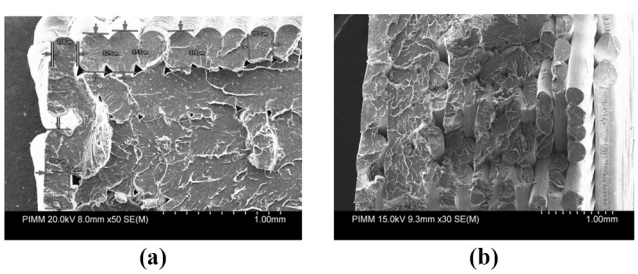

3.4.2 Effect of frequency

For different applied stresses (or amplitudes), the Wöhler curve obtained from fatigue tests in the case of PLA samples printed according to condition No. 3 in the frequencies of 1, 10 and 80 Hz as shown in Figure 13. Obviously, there is a small difference between the fatigue lifetime at mentioning frequencies at low amplitude while by increasing frequency, the curves shifted to low fatigue lifetime at high loading amplitude. According to Figure 13, one can note that the effect of frequency is more significant at loading stress from 35 MPa, which is corresponding to the damage threshold relating to Figure 9.

As an example, for applied stress of 40 MPa, the fatigue lifetime of the sample tested at 80 Hz is three times smaller than that of 1 Hz (respectively ~1,000 and ~3,000 cycles). This difference becomes more significant when the fatigue stress increases. It can be concluded that independent of the loading amplitudes, for values up to 1 Hz, frequency has a determinant role in the fatigue lifetime: increasing frequency decreases the fatigue lifetime. This phenomenon, in fact, is owing to the self-heating during the fatigue tests. Figure 14 shows the evolution of temperature as a function of time during fatigue test. One can observe the increase of about 3°C, at a loading amplitude of 31 MPa at the initial time of the test.

For the fatigue test at 1 Hz, self-heating is not significant while there is a slight increase in temperature at the frequency of 80 Hz (Figure 14). In this case, E/E_0 decreases by increasing the self-heating temperature. The slope of decreasing is increased by frequency augmentation. This phenomenon can be observed at low and high fatigue amplitudes. For high-frequency tests, the failure of the sample is because of both thermal fatigue and mechanical fatigue (Figure 15).

Figure 13 Wohler curves at different frequencies in tension-tension tests for PLA samples printed according to condition No. 3

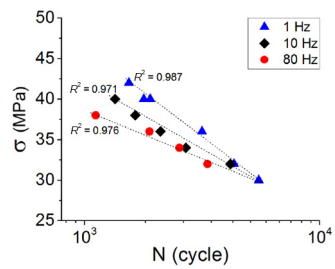

Figure 14 Self-heating curve during fatigue test of PLA samples printed according to condition No. 3

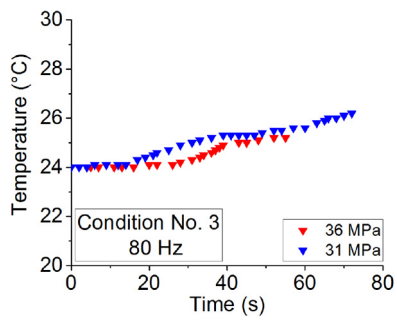

Figure 15 Evolution of the relative Young's modulus (E/E_0) during fatigue tests at different frequencies at (a) σ_{max} = 31 MPa (b) σ_{max} = 36 MPa

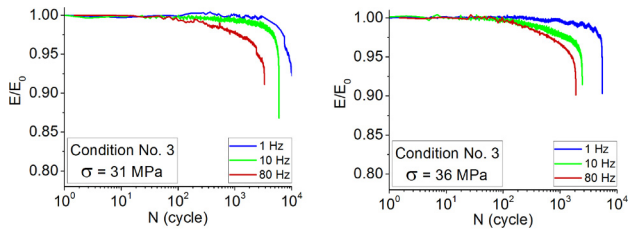

(a) (b)

In fact, SEM analysis of the samples tested at 80 Hz, highlights ductile behavior during loading. During the test at 10 Hz, the matrix remains brittle. The self-heating phenomenon causes the molecular motion to increase, the modulus decreases, and the polymer becomes softer. Moreover, one can observe from Figure 16(b) the change in rupture mode of PLA produced by FDM process. As indicated, inter-layer failure of the filaments and the transverse cracks exist.

4. Concluding remarks

The mechanical behavior of PLA specimens using FDM under both static and fatigue loadings is influenced mainly by the following parameters: filling temperature, filling rate, filling pattern, layer thickness, infill percentage, nozzle size and manufacturing orientation. According to the previous works (Vanaei *et al.*, 2020d), the temperature of extruder is the main parameter which influences the mechanical properties of PLA sample manufactured using FDM process.

In this paper, the mechanical properties of PLA specimens were tested to investigate the effect of extruder temperature. From this work, the obtained experimental results show the first observed damage phenomenon corresponds to the inter-layer bonding of the filament interface at the stress value of 40 MPa at the microscopic scale. A strong variation of fatigue lifetime as a function of the loading amplitude, frequency and extruder temperature is presented. For instance, fatigue lifetime is clearly dependent on the extruder temperature. Moreover, when the frequency is 80 Hz, self-heating decreased the fatigue lifetime which also depends on the coupling effect of thermal and mechanical fatigue. SEM observations demonstrated that the samples tested at 80 Hz, exhibited ductile behavior, whereas, the polymer remains brittle during the fatigue tests achieved at 1 Hz.

Figure 16 SEM micrographs after fatigue tests at 80 Hz and σ_{max} = 36 MPa for PLA samples printed according to condition No. 3: (a) and (b) show two views of observation

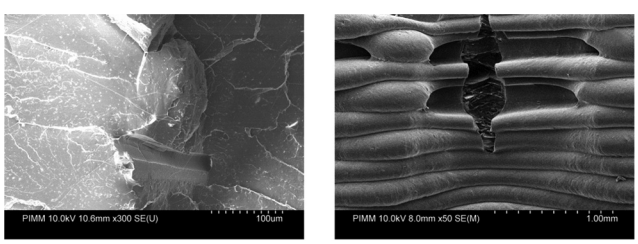

(a) (b)

As mentioned in this work during sample preparation, the pattern for each layer was selected to be printed in 45° to the axis X and Y (90° to each other's). This was to make sure that each successive layer has enough support on it. It means the best structural pattern. Nevertheless, the mechanical properties of the PLA samples printed by FDM process are limited. There are other process parameters to improve. Moreover, one can note that temperature analysis and control during FDM process should be performed (Vanaei *et al.*, 2020a).

References

Afrose, M.F., Masood, S., Iovenitti, P., Nikzad, M. and Sbarski, I. (2016), "Effects of part build orientations on fatigue behaviour of FDM-processed PLA material", *Progress in Additive Manufacturing*, Vol. 1 Nos 1/2, pp. 21-28.

Alhubail, M., Alenezi, D. and Aldousiri, B. (2013), "Taguchi-based optimisation of process parameters of fused deposition modelling for improved part quality", *International Journal of Engineering Research and Technology*, Vol. 2, p. 2519.

Averett, R.D., Realff, M.L., Jacob, K., Cakmak, M. and Yalcin, B. (2011), "The mechanical behavior of poly (lactic acid) unreinforced and nanocomposite films subjected to monotonic and fatigue loading conditions", *Journal of Composite Materials*, Vol. 45 No. 26, pp. 2717-2726.

Blattmeier, M., Witt, G., Wortberg, J., Eggert, J. and Toepker, J. (2012), "Influence of surface characteristics on fatigue behaviour of laser sintered plastics", *Rapid Prototyping Journal*, Vol. 18 No. 2, pp. 161-171.

Brandl, E., Heckenberger, U., Holzinger, V. and Buchbinder, D. (2012), "Additive manufactured AlSi10Mg samples using selective laser melting (SLM): microstructure, high cycle fatigue, and fracture behavior", *Materials & Design*, Vol. 34, pp. 159-169.

Chennakesava, P. and Narayan, Y.S. (2014), "Fused deposition modeling-insights", *Proceedings of the International Conference on Advances in Design and Manufacturing ICAD&M*, pp. 1345-1350.

Chua, C.K., Leong, K.F. and Lim, C.S. (2010), *Rapid Prototyping: principles and Applications (with Companion CD-ROM)*, World Scientific Publishing Company.

Crump, S.S. (1991), "Fast, precise, safe prototypes with FDM", *ASME annual winter conference, Atlanta*, 53-60.

Dong, Y., Ghataura, A., Takagi, H., Haroosh, H.J., Nakagaito, A.N. and Lau, K.-T. (2014), "Polylactic acid (PLA) biocomposites reinforced with coir fibres: evaluation of mechanical performance and multifunctional properties", *Composites Part A: Applied Science and Manufacturing*, Vol. 63, pp. 76-84.

Jerez-Mesa, R., Travieso-Rodriguez, J.A., Llumà-Fuentes, J., Gomez-Gras, G. and Puig, D. (2017), "Fatigue lifespan study of PLA parts obtained by additive manufacturing", *Procedia Manufacturing*, Vol. 13, pp. 872-879.

Kasuga, T., Ota, Y., Nogami, M. and Abe, Y. (2000), "Preparation and mechanical properties of polylactic acid composites containing hydroxyapatite fibers", *Biomaterials*, Vol. 22 No. 1, pp. 19-23.

Lee, J. and Huang, A. (2013), "Fatigue analysis of FDM materials", *Rapid Prototyping Journal*, Vol. 19 No. 4, pp. 291-299.

Letcher, T. and Waytashek, M. (2014), "Material property testing of 3D-printed specimen in PLA on an entry-level 3D printer", *ASME 2014 international mechanical engineering congress and exposition*, American Society of Mechanical Engineers, pp. V02AT02A014-V02AT02A014.

Macdonald, E., Salas, R., Espalin, D., Perez, M., Aguilera, E., Muse, D. and Wicker, R.B. (2014), "3D printing for the rapid prototyping of structural electronics", *IEEE Access*, Vol. 2, pp. 234-242.

Masood, S.H., Mau, K. and Song, W. (2010), "Tensile properties of processed FDM polycarbonate material", *Materials Science Forum*, Vols 654/656, pp. 2556-2559, Trans Tech Publ.

Mohamed, O.A., Masood, S.H. and Bhowmik, J.L. (2015), "Optimization of fused deposition modeling process parameters: a review of current research and future prospects", *Advances in Manufacturing*, Vol. 3 No. 1, pp. 42-53.

Santos, E., Abe, F., Kitamura, Y., Osakada, K. and Shiomi, M. (2002), "Mechanical properties of pure titanium models processed by selective laser melting", *Proceedings of the Solid Freeform Fabrication Symposium*, pp. 180-186.

Stephens, B., Azimi, P., EL Orch, Z. and Ramos, T. (2013), "Ultrafine particle emissions from desktop 3D printers", *Atmospheric Environment*, Vol. 79, pp. 334-339.

Susmel, L. (2014), "A unifying methodology to design un-notched plain and short-fibre/particle reinforced concretes against fatigue", *International Journal of Fatigue*, Vol. 61, pp. 226-243.

VAN Hooreweder, B., Moens, D., Boonen, R., Kruth, J.-P. and Sas, P. (2013), "On the difference in material structure and fatigue properties of nylon specimens produced by injection molding and selective laser sintering", *Polymer Testing*, Vol. 32 No. 5, pp. 972-981.

Vanaei, S., Parizi, M.S., Vanaei, S., Salemizadehparizi, F. and Vanaei, H.R. (2020), *An Overview on Materials and Techniques in 3D Bioprinting Toward Biomedical Application*, *Engineered Regeneration Journal*, available at: https://doi.org/10.1016/j.engreg.2020.12.001

Vanaei, H.R., Deligant, M., Shirinbayan, M., Raissi, K., Fitoussi, J., Khelladi, S. and Tcharkhtchi, A. (2020a), "A comparative in-process monitoring of temperature profile in fused filament fabrication", *Polymer Engineering & Science*, p. 9.

Vanaei, H.R., Raissi, K., Deligant, M., Shirinbayan, M., Fitoussi, J., Khelladi, S. and Tcharkhtchi, A. (2020b), "Toward the understanding of temperature effect on bonding strength, dimensions and geometry of 3D-printed parts", *Journal of Materials Science*, Vol. 55 No. 29, pp. 14677-14689.

Vanaei, H., Shirinbayan, M., Deligant, M., Raissi, K., Fitoussi, J., Khelladi, S. and Tcharkhtchi, A. (2020c), "Influence of process parameters on thermal and mechanical properties of polylactic acid fabricated by fused filament fabrication", *Polymer Engineering & Science*, Vol. 60, p. 10.

Vanaei, H.R., Shirinbayan, M., Costa, S.F., Duarte, F.M., Covas, J.A., Deligant, M., Khelladi, S. and Tcharkhtchi, A. (2020d), "Experimental study of PLA thermal behavior during fused filament fabrication", *Journal of Applied Polymer Science*, Vol. 138, p. 7.

Wang, F. (2012), "Mechanical property study on rapid additive layer manufacture Hastelloy® X alloy by selective laser melting technology", *The International Journal of Advanced Manufacturing Technology*, Vol. 58 Nos 5/8, pp. 545-551.

Yagnik, D. (2014), "Fused deposition modeling–a rapid prototyping technique for product cycle time reduction cost effectively in aerospace applications", *IOSR Journal of Mechanical and Civil Engineering*, Vol. 5, pp. 62-68.

Corresponding author

Hamid Reza Vanaei can be contacted at: hamidreza.vanaei@ensam.eu